ISSN 1070-3284, Russian Journal of Coordination Chemistry, 2022, Vol. 48, No. 5, pp. 278–286. © Pleiades Publishing, Ltd., 2022.
Russian Text © The Author(s), 2022, published in Koordinatsionnaya Khimiya, 2022, Vol. 48, No. 5, pp. 277–286.

# Heterometallic Germanium(IV) Complexes Based on the *N*-Phenyl-Substituted *o*-Amidophenolate Ligand

**A. V. Piskunov[a], *, K. V. Arsenyeva[a], A. V. Klimashevskaya[a], and A. V. Cherkasov[a]**

[a] *Razuvaev Institute of Organometallic Chemistry, Russian Academy of Sciences, Nizhny Novgorod, Russia*

**e-mail: pial@iomc.ras.ru*

Received October 27, 2021; revised November 3, 2021; accepted November 6, 2021

**Abstract**—New bimetallic complexes $^{Ph}$APGe[M(CO)$_n$Cp]$_2$ ($^{Ph}$AP is 3,5-di-*tert*-butyl-*N*-(phenyl)-*o*-aminophenolate dianion; M = Fe, *n* = 2 (**II**); M = W, *n* = 3 (**III**)) are synthesized by the insertion of O,N-heterocyclic germylene $^{Ph}$APGe (**I**) at the metal–metal bond in dimers [Fe(CO)$_2$Cp]$_2$ and [W(CO)$_3$Cp]$_2$. The oxidation of compounds **II** and **III** with silver(I) triflate affords paramagnetic germanium(IV) *o*-iminosemiquinolates detected by EPR spectroscopy. The oxidative addition of 3,6-di-*tert*-butyl-*o*-benzoquinone to germylene **I** proceeds via the oxidation of the low-valence center to the tetravalent state and is accompanied by symmetrization with the formation of the corresponding bis-*o*-amidophenolate and bis(catecholate) derivatives of germanium(IV). Digermylene oxide **Ia** synthesized by the hydrolysis of starting germylene **I** acts as the oxidant in the reaction with the nickel cyclopentadienylcarbonyl dimer and forms an eight-membered metallocycle supporting four Ge(II)–Ni(II) donor–acceptor bonds in compound (CpNi)$_2$[$^{Ph}$APGeOGe$^{Ph}$AmP]$_2$ ($^{Ph}$AmP is 3,5-di-*tert*-butyl-*N*-(phenyl)-*o*-aminophenolate anion) (**IV**). The molecular structures of compounds **II**–**IV** are determined by X-ray diffraction (XRD) (CIF files CCDC nos. 2118153–2118155, respectively).

**Keywords:** germanium, oxidative addition, XRD, electron paramagnetic resonance

**DOI:** 10.1134/S1070328422050074

## INTRODUCTION

Coordination and organometallic compounds containing redox-active ligands are among promising trends for the development of the modern chemistry. They find application in many fields of research, such as catalytic transformations of small molecules, molecular electronics, and molecular magnetism [1–4]. Interest in ligands of this type is caused by the ability to undergo reversible redox transformations retaining the bond with the metal. The chemistry of metal complexes containing ligands of this type is intensively developed predominantly for the transition metal derivatives [5–8]. Some of these compounds have unique magnetic and electronic properties [9–13]. Paramagnetic radical-anion forms of redox-active ligands can successfully be applied as spin-labeled ligands [14]. The EPR spectra of these compounds are highly informative and can provide diverse data on their structures and transformation mechanisms in solutions [15–21].

A new trend for inserting the main group elements in complexes with redox-active ligands has been developed in the recent years. This combination makes it possible to involve such compounds in oxidative addition and reductive elimination reactions without changing the oxidation state of the complex-forming agent [1, 22–24] and to observe weak magnetic interactions that are not complicated by the presence of a paramagnetic transition metal ion [25]. Many researchers make attempts to synthesize heterometallic derivatives with the direct formation of the metal–metal bond from redox-active ligand systems. In these compounds, the nontransition metal atom of predominantly groups 13 [26–32] or 14 [33–38] is covalently bound to the transition metal or lanthanide [29, 39–41]. The prevailing number of such studies was carried out for the redox-active diimine ligands. Only in several works the nontransition metal atom is chelated by diolate [35, 42] or amidophenolate [43, 44] ligands. As a rule, the redox properties of organic ligands in compounds of this type were not studied.

In this work we describe the synthesis and chemical behaviour of organobimetallic derivatives with Ge–M bonds (M = Fe, Ni, W) involved redox-active 3,5-di-*tert*-butyl-*N*-(phenyl)-*o*-amidophenolate ligand.

## EXPERIMENTAL

All procedures on the synthesis and study of chemical transformations of the germanium complexes were carried out in the absence of air oxygen and moisture. The solvents used were purified and dehydrated according to published recommendations [45].

Commercial reagent $[CpFe(CO)_2]_2$ was applied. Germanium *o*-amidophenolate (**I**) and germanium *o*-amidophenolate oxide (**Ia**) were synthesized according to described procedures [43, 46]. The nickel cyclopentadienylcarbonyl [47] and tungsten cyclopentadienylcarbonyl [48] dimers were synthesized according to known methods.

NMR spectra were recorded using a Bruker Avance Neo 300 MHz spectrometer. EPR spectra were detected on a Bruker EMX spectrometer. 2,2-Diphenyl-1-picrylhydrazyl ($g$ = 2.0037) served as the standard for $g$ factor determination. To determine the precise parameters, the EPR spectrum was simulated using the WinEPR SimFonia program (Bruker).

**Synthesis of complexes ($^{Ph}$AP)Ge[Fe(CO)$_2$Cp]$_2$ (II) and ($^{Ph}$AP)Ge[W(CO)$_3$Cp]$_2$ (III).** A pale yellow solution of germylene **I** (0.4 mmol, 0.15 g) in THF was added to a equimolar quantity of $[CpM(CO)_n]_2$ (0.4 mmol; M = Fe ($n$ = 2), 0.14 g; M = W ($n$ = 3), 0.27 g) inducing an almost instant color change to intensive vinous, and the reaction mixture was left to stay at room temperature with vigorous stirring for 12 h. Complexes **II** and **III** were isolated as diamagnetic dark red crystalline substances from a concentrated solution in hexane at room temperature.

Complex **II**. The yield was 0.22 g (0.31 mmol, 78%). $^1$H NMR ($C_6D_6$; 20°C; δ, ppm): 7.6 (d, 2H, $H_{Ph}$, $J_{H,H}$ = 7.7 Hz); 7.52 (d, 1H, $H_{AP}$, $J_{H,H}$ = 2.2 Hz); 7.1 (d, 1H, $H_{AP}$, $J_{H,H}$ = 2.2 Hz); 7.33 (m, 2H, $H_{Ph}$); 6.95 (m, 1H, $H_{Ph}$); 4.2 (s, 10H, Cp); 1.8 (s, 9H, *t*-Bu); 1.38 (s, 9H, *t*-Bu). $^{13}$C NMR ($C_6D$; 20°C; δ, ppm): 214.3, 213.3 (C≡O); 152.4, 148.4, 139.6, 122.0, 121,1 ($C_{Ph}$); 139.2 (N–$C_{Ph}$); 133.5 (C–N); 129.4 (C–O); 83.3 (Cp); 34.9, 34.2 ($C_{quater}$); 29.8, 31.8 ($C_{t\text{-}Bu}$).

Complex **III**. The yield was 0.26 g (0.25 mmol, 63%). $^1$H NMR ($C_6D_6$; 20°C; δ, ppm): 7.63 (d, 1H, $H_{AP}$, $J_{H,H}$ = 2.2 Hz); 7.61 (d, 1H, $H_{AP}$, $J_{H,H}$ = 2.2 Hz); 7.44 (s, 1H, $H_{Ph}$); 7.34 (m, 2H, $H_{Ph}$); 7.01 (m, 2H, $H_{Ph}$); 4.81 (s, 10H, Cp); 1.82 (s, 9H, *t*-Bu); 1.38 (s, 9H, *t*-Bu). $^{13}$C NMR ($C_6D_6$; 20°C; δ, ppm): 220.4, 217.7, 217.5 (C≡O); 151.6, 147.7, 140.3, 123.2, 121,8 ($C_{Ph}$); 139.8 (N–$C_{Ph}$); 133.5 (C–N); 129.5 (C–O); 90.23 (Cp); 34.95, 34.48 ($C_{quater}$); 31.8, 30.1 ($C_{t\text{-}Bu}$).

**Synthesis of complex (CpNi)$_2$[$^{Ph}$APGeOGe$^{Ph}$AmP]$_2$ (IV).** A solution of $[CpNiCO]_2$ (0.042 g, 0.138 mmol) in toluene (10 mL) was added to a solution of digermylene oxide **Ia** (0.138 mmol) obtained in situ in the same solvent (10 mL). The reaction mixture was stored at room temperature in the dark for 2 days. The color of the solution changed to brown within this time. Complex **IV** was isolated as a yellow crystalline powder after the solvent was replaced by hexane. The yield was 0.22 g (0.07 mmol, 52%).

$^1$H NMR ($C_6D_6$; 20°C; δ, ppm): 7.71 (d, 1H, $H_{AP}$, $J_{H,H}$ = 2.2 Hz); 7.59 (d, 1H, $H_{AP}$, $J_{H,H}$ = 2.0 Hz); 7.35–6.66 (m, 12H, $H_{Ph}$, NH); 6.65 (d, 1 H, $H_{AP}$, $J_{H,H}$ = 2.2 Hz), 6.44 (d, 1 H, $H_{AP}$, $J_{H,H}$ = 2.0 Hz), 4.99 (s, 10H, Cp), 1.47 (s, 9H, *t*-Bu), 1.34 (s, 9H, *t*-Bu), 1.19 (s, 9 H, *t*-Bu), 1.04 (s, 9 H, *t*-Bu).

**Reaction of complex I with 3,6-di-*tert*-butyl-*o*-benzoquinone.** A solution of quinone (0.119 g, 0.54 mmol) in THF (10 mL) was slowly poured to a solution of germylene **I** (0.2 g, 0.54 mmol) in toluene (10 mL). The reaction mixture rapidly turned brown. The solvent was removed under reduced pressure, and the residue was dissolved in dichloromethane. The addition of hexane to the obtained mixture resulted in the formation of a white crystalline precipitate of bis(3,6-di-*tert*-butylcatecholato)germanium(IV) ditetrahydrofuranate (**V**) described previously according to the $^1$H and $^{13}$C spectroscopy data [49]. The yield was 0.095 g (0.18 mmol, 34%).

**XRD** of compounds **II**, **III**, and **IV** was carried out on a Bruker D8 Quest diffractometer (ω scan mode, Mo$K_\alpha$ radiation, λ = 0.71073 Å). Experimental sets of intensities were measured and integrated, an absorption correction was applied, and structure refinement was performed using the APEX3 [50], SADABS [51], and SHELX [52] program packages. The structures were solved using the dual-space algorithm [53] and refined by full-matrix least squares for $F^2_{hkl}$ in the anisotropic approximation for non-hydrogen atoms. The hydrogen atom H(1*A*) in compound **IV** was found from the difference electron density Fourier synthesis. All other hydrogen atoms in compounds **II**, **III**, and **IV** were placed in the geometrically calculated positions and refined isotropically with fixed thermal parameters $U(H)_{iso}$ = $1.2U(C)_{equiv}$ ($U(H)_{iso}$ = $1.5U(C)_{equiv}$ for methyl fragments). The crystallographic data and experimental XRD and structure refinement parameters are given in Table 1.

The structures were deposited with the Cambridge Crystallographic Data Centre (CIF files CCDC nos. 2118153 (**II**), 2118154 (**III**), and 2118155 (**IV**); ccdc.cam.ac.uk/structures).

## RESULTS AND DISCUSSION

The insertion of low-valence derivatives of group 14 elements at the metal–metal bond is a reliable and popular method for the synthesis of heterometallic derivatives with the transition metal–tetrylene bond [35, 54]. We found that the reactions of monomeric germanium(II) amidophenolate **I** with cyclopentadienylcarbonyls of transition metals $[CpM(CO)_n]_2$ (M = Fe, $n$ = 2; M = W, $n$ = 3) afforded new bimetallic complexes (**II**, **III**) in good yields according to Scheme 1. The reaction completely ceased within 24 h at room temperature in a toluene solution. The final compounds were isolated as solid dark brown crystalline products. Compounds **II** and **III** in the crystalline state are stable in air for several days, but their solu-

**Table 1.** Crystallographic data and structure refinement parameters for compounds **II**, **III**, and **IV**

| Parameter | Value | | |
|---|---|---|---|
| | **II** | **III** | **IV** |
| Empirical formula | $C_{34}H_{35}NO_5Fe_2Ge$ | $C_{36}H_{35}NO_7GeW_2$, $1/2C_6H_{14}$ | $C_{90}H_{112}N_4Ni_2Ge_4O_6$, $C_6H_{14}$ |
| *FW* | 721.92 | 1077.02 | 1839.78 |
| Crystal system | Monoclinic | Monoclinic | Triclinic |
| Space group | $P2_1/n$ | $P2_1/c$ | $P\bar{1}$ |
| *T*, K | 100 | 120 | 100 |
| *a*, Å | 13.7818(5) | 13.1443(5) | 10.0556(9) |
| *b*, Å | 12.4681(4) | 17.8359(8) | 12.9106(11) |
| *c*, Å | 18.7331(6) | 16.8068(7) | 19.0244(16) |
| α, deg | 90 | 90 | 75.069(3) |
| β, deg | 105.074(2) | 104.8300(10) | 75.495(3) |
| γ, deg | 90 | 90 | 79.371(3) |
| *V*, Å$^3$ | 3108.20(18) | 3808.9(3) | 2291.3(3) |
| *Z* | 4 | 4 | 1 |
| $\rho_{calc}$, g/cm$^3$ | 1.543 | 1.878 | 1.333 |
| μ, mm$^{-1}$ | 1.925 | 6.858 | 1.751 |
| Crystal size, mm | 0.34 × 0.21 × 0.05 | 0.19 × 0.11 × 0.04 | 0.26 × 0.09 × 0.03 |
| Scan range over θ, deg | 2.12–30.20 | 2.10–26.10 | 2.17–25.08 |
| Number of measured/ independent reflections | 33210/9204 | 45580/7552 | 25909/8064 |
| $R_{int}$ | 0.0565 | 0.0676 | 0.0756 |
| Number of independent reflections with $I > 2\sigma(I)$ | 6944 | 5955 | 5652 |
| Number of refined parameters/restraints | 394 | 488 | 682 |
| $R$ ($I > 2\sigma(I)$) | $R_1 = 0.0429$, $wR_2 = 0.0901$ | $R_1 = 0.0401$, $wR_2 = 0.0646$ | $R_1 = 0.0606$, $wR_2 = 0.1008$ |
| $R$ (for all data) | $R_1 = 0.0709$, $wR_2 = 0.0990$ | $R_1 = 0.0614$, $wR_2 = 0.0697$ | $R_1 = 0.1030$, $wR_2 = 0.1179$ |
| $S$ ($F^2$) | 1.016 | 1.020 | 1.056 |
| Maximum and minimum of residual electron density, e Å$^{-3}$ | 0.99/–0.50 | 1.41/–0.91 | 0.84/–0.68 |

tions slowly decompose in aerobic atmosphere. Under similar conditions, the reaction of germylene **I** involving nickel compound $[CpNi(CO)]_2$ is not accompanied by a visible color change of the reaction mixture. We failed to isolate and characterize individual substances from this reaction mixture.

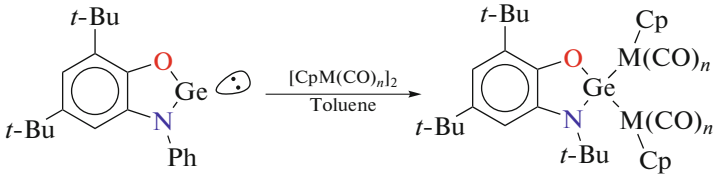


**(I)**

M: Fe, $n = 2$ (**II**)
M: W, $n = 3$ (**III**)

**Scheme 1.**

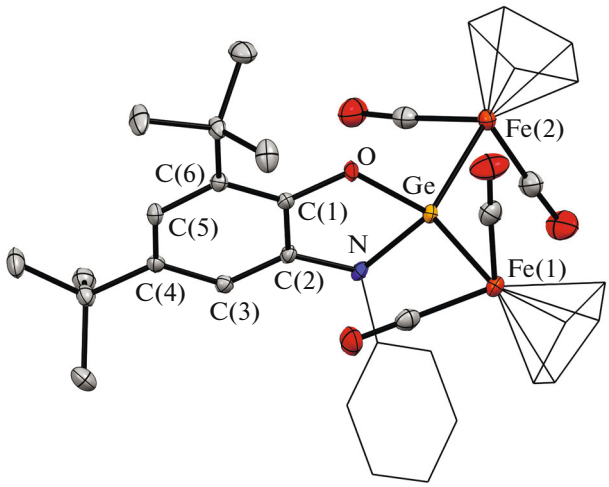


**Fig. 1.** Molecular structure of complex $^{Ph}$APGe[CpFe(CO)$_2$]$_2$ (**II**). Thermal ellipsoids of selected atoms are given with 50% probability. Hydrogen atoms are omitted for clarity.

The formation of diamagnetic amidophenolate complexes **II** and **III** is confirmed by the $^1$H and $^{13}$C NMR spectroscopy data. The spectra demonstrate a well resolved spectrum at room temperature in which the single additional signal corresponding to the cyclopentadienyl substituents is observed along with the protons of the *o*-amidophenolate fragment. The $^{13}$C NMR spectrum in the diagnostic range of carbonyl carbon atoms shows only two peaks for compound **II** and three peaks for compound **III**. This indicates that two fragments with transition metals in the coordination sphere of the Ge atom are equivalent in solutions of complexes **II** and **III**.

We carried out single-crystal XRD studies of complexes **II** and **III**. According to the data obtained, the coordination polyhedra of the germanium atoms in these compounds are distorted tetrahedra. The molecular structures of compounds **II** and **III** are similar and presented in Figs. 1 and 2, respectively, and selected bond lengths and angles in these complexes are given in Table 2. In each complex the amidophenolate fragment $^{R}$APGe is bonded to two CpM(CO)$_n$ fragments (M = Fe, $n$ = 2 for **II**; M = W, $n$ = 3 for **III**) due to the Ge–M bond. The OGeN angles (87.09(8)° (**II**) and 86.4(2)° (**III**)) are typical of similar Ge(IV) derivatives [55] and are only slightly larger than an analogous angle in starting complex **I** (85.95(9)°) [43]. The C–O (1.367(2) (**II**), 1.371(7) (**III**) Å) and C–N (1.414(3) (**II**), 1.395(8) (**III**) Å) bond lengths in the amidophenolate ligands lie in a characteristic range of 1.35–1.42 Å and are comparable with analogous values in amidophenolates of tetravalent metals. On the whole, the geometric parameters of this ligand are typical of the O,N-coordinated amidophenolate dianions [55–58]. The WGeW angle (127.06(2)°) in compound **III** is somewhat larger than FeGeFe (123.02(2)°) in compound **II** and is caused, most likely, by a higher steric hindrance of the coordination sphere due to more bulky organometallic fragments CpW(CO)$_3$ compared to CpFe(CO)$_2$. The Ge–Fe bond lengths in compound **II** are 2.3782(4) and 2.3867(4) Å. The Ge–W distances (2.6987(7), 2.7027(7) Å) in compound **III** only slightly differ from those in [CpW(CO)$_3$]$_2$GeCl$_2$ [59].

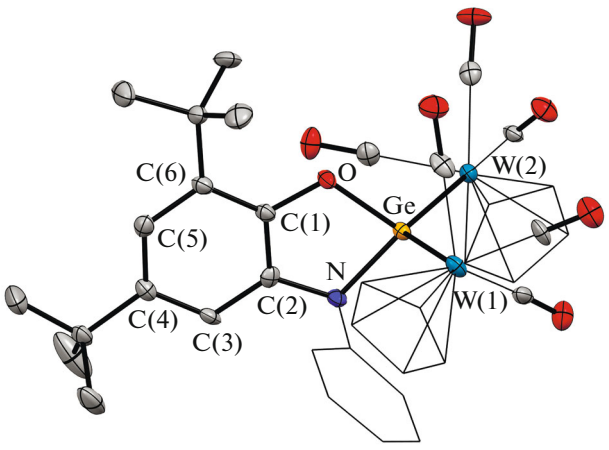


**Fig. 2.** Molecular structure of complex $^{Ph}$APGe[CpW(CO)$_3$]$_2$ (**III**). Thermal ellipsoids of selected atoms are given with 50% probability. Hydrogen atoms are omitted for clarity.

We showed [46] that germylene **I** did not react with electron-unsaturated vanadocene. At the same time, this metallocene reacts easily with digermylene oxide **Ia** formed upon the careful hydrolysis of compound **I**. The reaction of compound **Ia** (synthesized in situ according to a known procedure [46]) with

**Table 2.** Selected bond lengths and angles for compounds **II** and **III**

| Bond | **II** | **III** |
|---|---|---|
| | *d*, Å | |
| Ge–N | 1.921(2) | 1.909(5) |
| Ge–O | 1.849(2) | 1.854(4) |
| C(1)–O | 1.367(3) | 1.371(7) |
| C(2)–N | 1.414(3) | 1.395(8) |
| C(1)–C(2) | 1.403(3) | 1.395(8) |
| C(2)–C(3) | 1.385(3) | 1.412(8) |
| C(3)–C(4) | 1.401(3) | 1.399(9) |
| C(4)–C(5) | 1.391(3) | 1.374(9) |
| C(5)–C(6) | 1.406(3) | 1.407(8) |
| C(6)–C(1) | 1.403(3) | 1.396(8) |
| Ge–W(1) | | 2.6987(7) |
| Ge–W(2) | | 2.7027(7) |
| Ge–Fe(1) | 2.3782(4) | |
| Ge–Fe(2) | 2.3867(4) | |
| Angle | ω, deg | |
| OGeN | 87.09(8) | 86.4(2) |
| OGeM(1) | 106.63(5) | 112.1(2) |
| NGeM(1) | 113.96(6) | 111.5(2) |
| OGeM(2) | 107.85(5) | 100.8(2) |
| NGeM(2) | 111.75(6) | 111.5(2) |
| M(1)GeM(2) | 123.02(2) | 127.06(2) |

$[CpNiCO]_2$ occurs slowly at room temperature under mild conditions (Scheme 2). During the reaction the intensive red color of $[CpNiCO]_2$ changes to yellow-brown. As a result, germanium–nickel complex **IV** was isolated from the reaction mixture as a yellow crystalline substance.

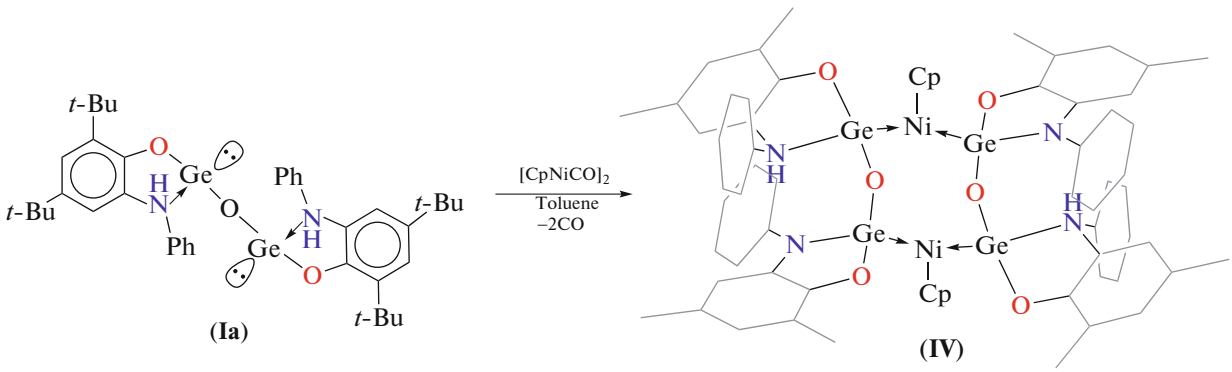


**Scheme 2.**

The molecular structure of compound **IV** is shown in Fig. 3 and represents a dimeric heterobimetallic complex of nickel(II) and germanium(II) in which each nickel atom is linked with one cyclopentadienyl ligand and two digermylene oxide anionic fragments. In this reaction, the $Ni^{+}$ ion (Scheme 2) reduces one of the aminophenolate protons of digermylene **Ia** with the oxidation to the $Ni^{2+}$ ion. As a consequence, one of the aminophenolate fragments is transformed to the amidophenolate state, whereas the second germanium

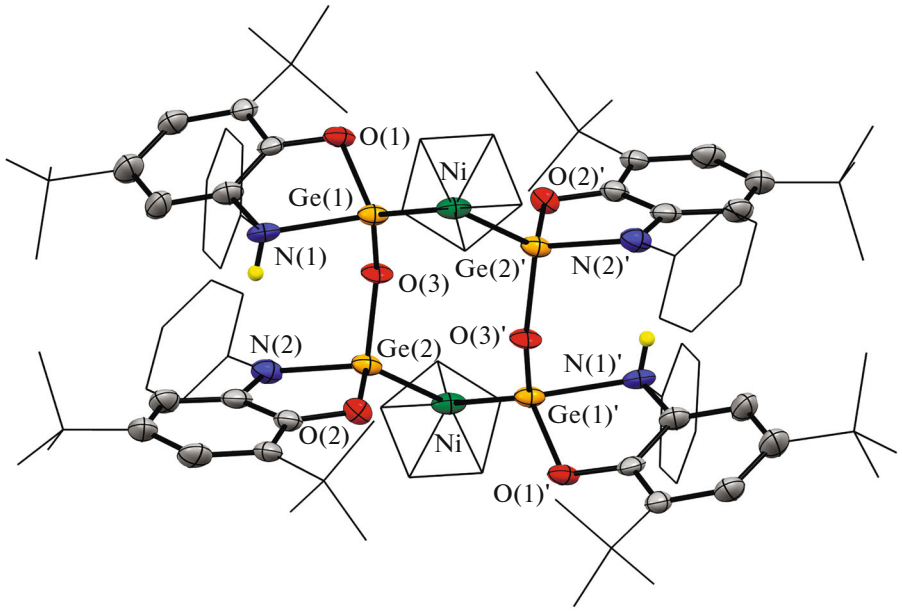


**Fig. 3.** Molecular structure of complex $(CpNi)_2[^{Ph}APGeOGe^{Ph}AmP]_2$ (**IV**). Thermal ellipsoids of selected atoms are given with 50% probability. Hydrogen atoms are omitted for clarity.

center of digermylene oxide remains unchanged. The formal coordination numbers $CN_{Ge(II)}$ and $CN_{Ni(II)}$ in compound **IV** are 4 and 5, respectively.

In the formed eight-membered metallocycle existing in the twist conformation, both low-valence germanium(II) atoms are bound to the cationic nickel centers due to the donor–acceptor interaction. The Ni–Ge distances in compound **IV** are comparable: the length of the Ge(2) → Ni bond formed by anionic germylene with the deprotonated organic ligand is 2.2129(9) Å, which is slightly shorter than the Ge(1)–Ni distance (2.2229(9) Å). Thus, the distribution of the Ni–Ge bond lengths in the metallocycle indicates the electron density delocalization over the GeNiGe fragment. It is important that the Ge–Ni bonds in compound **IV** are appreciably shorter than the values observed for the known structures containing the Ge–Ni–Cp fragment (~2.3 Å) [60, 61]. At the same time, they are substantially longer that the donor–acceptor bond (2.08 Å) formed upon the interaction of the cyclopentadienylnickel center with *N*,*N*-heterocyclic diamidogermylene [62]. The observed difference is caused by the higher $CN_{Ge}$ in compound **IV** compared to that of the nickel complex [62].

**Table 3.** Selected bond lengths in the amidophenolate ($^{Ph}AP$) and aminophenolate ($^{Ph}AmP$) fragments of compound **IV**

| Bond | $^{Ph}AP$ | $^{Ph}AmP$ |
|---|---|---|
| | *d*, Å | |
| Ge–N | 1.887(4) | 2.124(5) |
| Ge–O | 1.837(3) | 1.838(3) |
| C–O | 1.364(6) | 1.368(6) |
| C–N | 1.409(7) | 1.473(7) |
| Ge–Ni | 2.2289(9) | 2.2129(9) |
| $Ge–O_{oxide}$ | 1.787(3) | 1.745(3) |

A substantial difference in geometry is distinctly observed between two germanium fragments in compound **IV** (comparative analysis of the bond lengths in these fragments is given in Table 3). An inflection along the O...N line is observed in the Ge(1)O(1)C(1)C(2)N(1) metallocycle of the protonated aminophenolate fragment $^{Ph}AmP$ (the dihedral angle between two planes O(1)Ge(1)N(1) and O(1)C(1)C(2)N(1) is 26.1(2)°), whereas the metallocycle in the amidophenolate fragment is nearly planar (6.6(2)°). In addition, the protonated nitrogen atom N(1) has a characteristic tetrahedral environment compared to the amidophenolate N(2) atom. The coordination Ge(1)–N(1) bond (2.124(5) Å) is noticeably longer than the covalent Ge(2)–N(2) bond (1.887(4) Å). The Ge–O distances are nearly equal to each other (1.834(3), 1.837(3) Å) and considerably exceed analogous distances in tetrahedral germanium(IV) bis(amidophenolate) [55]. All these data confirm that the low oxidation state of the germanium atoms is retained in compound **IV**.

Each of the nickel atoms in compound **IV** has a distorted planar trigonal coordination environment, and the germanium atoms and centroid of the cyclopentadienyl ligand occupy the vertices. The deviation of Ni(II) from the $Ge(1)Cp_{center}Ge(2)$ plane is 0.34 Å.

The distance between the nickel atoms in compound **IV** is 6.036(2) Å, which excludes valence interactions between them. The Ni–$Cp_{center}$ bond length is 1.714(2) Å, which is considerably shorter than similar distances in nickelocene (2.14–2.18 Å).

Heterometallic complex **IV** has a well resolved $^1$H NMR spectrum in which the protons of the cyclopentadienyl group are observed as a singlet at 4.99 ppm. The $^{13}$C NMR spectrum was not obtained because of an insufficient solubility of complex **IV**.

It was found that compounds **II** and **III** can undergo one-electron oxidation with silver triflate including the redox-active amidophenolate ligand to form the paramagnetic Ge(IV) *o*-iminosemiquinone derivatives (Scheme 3).

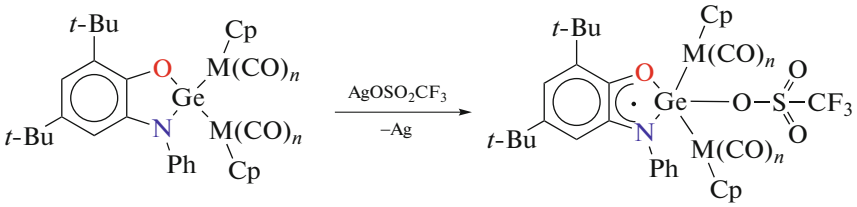


M: Fe, $n = 2$ (**II**)
M: W, $n = 3$ (**III**)

M: Fe, $n = 2$ (**VI**)
M: W, $n = 3$ (**VII**)

**Scheme 3.**

The reaction is accompanied by the precipitation of metallic silver and a color change of the reaction mixture from dark red to intensive violet. The EPR spectrum exhibits intense signals indicating the oxidation of the amidophenolate ligand to the paramagnetic form (Fig. 4). The hyperfine structure of the spectrum (doublet (1 : 1) of triplets (1 : 1 : 1)) is caused by the hyperfine interaction of the unpaired electron with one proton and one nitrogen atom of the *o*-iminosemiquinonate ligand. However, the intensively colored reaction mixture rather rapidly loses color, and the paramagnetic bimetallic derivatives decompose in the solution. It was impossible to isolate them in the individual state. In the case of tungsten compound **VII**, impurity signals are observed in the EPR spectrum even at the first steps of the reaction, indicating its higher lability compared to less sterically hindered complex **VI**.

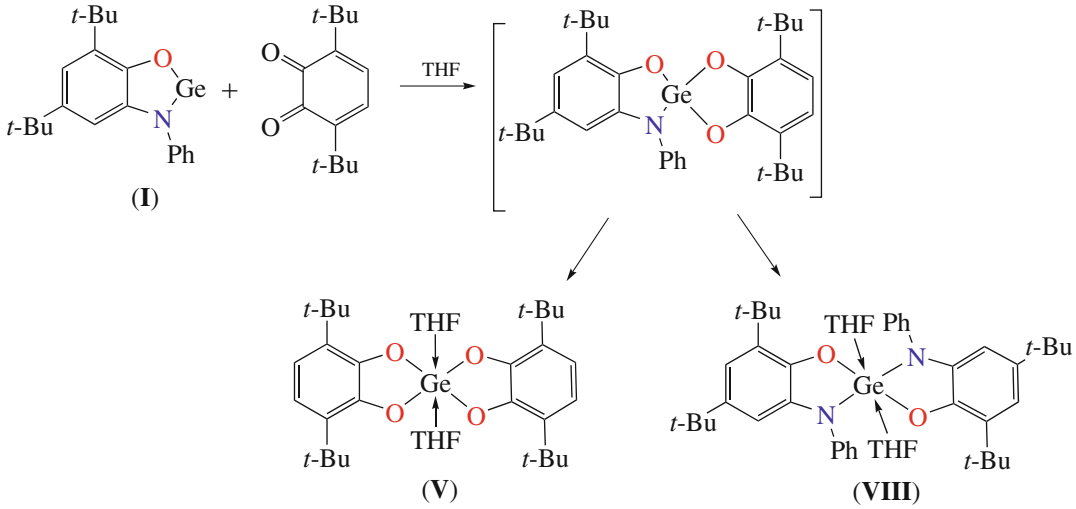


(**I**) (**V**) (**VIII**)

**Scheme 4.**

The germanium(II) and tin(II) derivatives based on the redox-active ligands can enter into the redox reactions involving both the organic fragment and low-valence tetrylene center [57, 58]. It was expected that the oxidative addition of 3,6-di-*tert*-butyl-*o*-benzoquinone to the low-valence metal center of germylene **I** would make it possible to obtain a heteroligand derivative of tetravalent germanium containing redox-active dianions of two types: catecholate and *o*-amidophenolate. The reaction occurs in a THF solution with the rate of mixing reactants (Scheme 4). However, only symmetrical bis(3,6-di-*tert*-butylcatecholato)germanium(IV) bis(tetrahydrofuranate) (**V**) was isolated by crystallization from the reaction mixture.

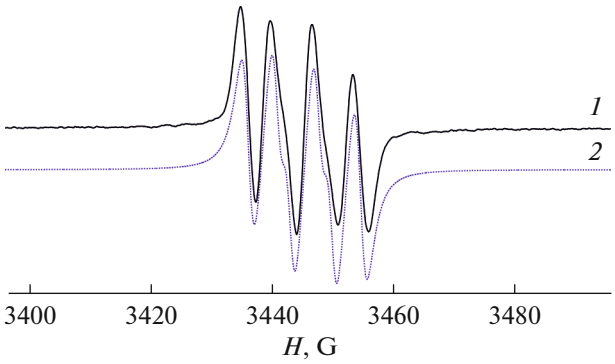


**Fig. 4.** (*1*) Experimental and (*2*) simulated isotropic EPR spectra of compound **VI** in toluene. Spectral parameters: $a_i$(H) = 4.7 G, $a_i$($^{14}$N) = 6.9 G, and $g_i$ = 2.0032.

The structural and spectral characteristics of compound **V** correspond to previously published data [49]. This indicates the symmetrization in a solution of the unsymmetric derivative with the formation of compounds **VIII** and **V**.

Thus, new heterometallic complexes with the Ge–M bonds (M = Fe, W, Ni) were synthesized by the insertion of the low-valence germanium(II) derivative bearing the 3,5-di-*tert*-butyl-*N*-phenyl-*o*-amidophenolate ligand at the M–M bond in dimers of transition metal cyclopentadienylcarbonyls. The one-electron oxidation of the new organobimetallic compounds with silver triflate gives the unstable paramagnetic *o*-iminosemiquinolate germanium(IV) derivatives. The two-electron oxidation of germylene with *o*-quinone affords the unstable heteroligand intermediate that undergoes symmetrization.

## ACKNOWLEDGMENTS

This work was carried out using the equipment of the Center for Collective Use "Analytical Center of the Razuvaev Institute of Organometallic Chemistry of the Russian Academy of Sciences" supported by the grant "Provision of Development of Material Technical Infrastructure of Centers for Collective Use of Scientific Equipment" (unique identifier RF 2296.61321X0017, agreement no. 075-15-2021-670).

## FUNDING

The study was supported by the Russian Science Foundation, project no. 17-13-01428p.

## CONFLICT OF INTEREST

The authors declare that they have no conflicts of interest.

## REFERENCES

1. Abakumov, G.A., Piskunov, A.V., Cherkasov, V.K., et al., *Russ. Chem. Rev.*, 2018, vol. 87, no. 5, p. 393.
2. Luca, O.R. and Crabtree, R.H., *Chem. Soc. Rev.*, 2012, vol. 42, no. 4, p. 1440.
3. Bas de Bruin, Gualco, P., and Paul, N.D., *Ligand Design in Metal Chemistry: Reactivity and Catalysis*, New York: Wiley, 2016, p. 448.
4. Schulz, S., *Chem. - Eur. J.*, 2010, vol. 22, no. 16, p. 6416.
5. Poddel'sky, A.I., Cherkasov, V.K., and Abakumov, G.A., *Coord. Chem. Rev.*, 2009, vol. 253, p. 291.
6. Kaim, W., *Inorg. Chem.*, 2011, vol. 50, p. 9752.
7. Starikova, A.A. and Minkin, V.I, *Russ. Chem. Rev.*, 2018, vol. 87, p. 1049.
8. Fomenko, I.S. and Gushchin, A.L., *Russ. Chem. Rev.*, 2020, vol. 89, p. 966.
9. Dei, A., Gatteschi, D., Sangregorio, C., and Sorace, L., *Acc. Chem. Res.*, 2004, vol. 37, p. 827.
10. Markevtsev, I.N., Monakhov, M.P., Platonov, V.V., et al., *J. Magn. Magn. Mater.*, 2006, vol. 300, p. e407.
11. Sato, O., *J. Photochem. Photobiol.*, 2004, vol. 5, p. 203.
12. Abakumov, G.A., Cherkasov, V.K., Nevodchikov, V.I., et al., *Inorg. Chem.*, 2001, vol. 40, p. 2434.
13. Pierpont, C.G., *Coord. Chem. Rev.*, 2001, vols. 216–217, p. 99.
14. Abakumov, G.A., *Zh. Vsesoyuz. Khim. ob-va im. D.I. Mendeleeva*, 1979, vol. 17, p. 156.
15. Kozhanov, K.A., Bubnov, M.P., Cherkasov, V.K., et al., *Dalton Trans.*, 2004, p. 2957.
16. Piskunov, A.V., Tsys, K.V., Cherkasov, A.V., and Chegerev, M.G., *Russ. J. Coord. Chem.*, 2019, vol. 45, p. 626. https://doi.org/10.1134/S0132344X19090068
17. Meshcheryakova, I.N., Arsenyeva, K.V., Fukin, G.K., et al., *Mendeleev Commun.*, 2020, vol. 30, no. 5, p. 592.
18. Bubnov, M.P., Kozhanov, K.A., Skorodumova, N.A., et al., *J. Mol. Struct.*, 2019, vol. 1180, p. 878.
19. Kozhanov, K.A., Bubnov, M.P., Teplova, I.A., et al., *J. Mol. Struct.*, 2017, vol. 1147, p. 541.
20. Kozhanov, K.A., Bubnov, M.P., Abakumov, G.A., and Cherkasov, V.K., *J. Magn. Reson.*, 2012, vol. 225, p. 62.
21. Bubnov, M.P., Teplova, I.A., Kozhanov, K.A., et al., *J. Magn. Reson.*, 2011, vol. 209, no. 2, p. 149.
22. Ershova, I.V. and Piskunov, A.V., *Russ. J. Coord. Chem.*, 2020, vol. 46, p. 154. https://doi.org/10.1134/S1070328420030021
23. Chegerev, M.G. and Piskunov, A.V., *Russ. J. Coord. Chem.*, 2018, vol. 44, p. 258. https://doi.org/10.1134/S1070328418040036
24. Broere, D.L., Plessius, R., and van der Vlugt, J.I., *Chem. Soc. Rev.*, 2015, vol. 44, p. 6886.
25. Ershova, I.V., Piskunov, A.V., and Cherkasov, V.K., *Russ. Chem. Rev.*, 2020, vol. 89, p. 1157.
26. Dange, D., Choong, S.L., Schenk, C., et al., *Dalton Trans.*, 2012, vol. 41, p. 9304.
27. Protchenko, A.V., Saleh, L.M.A., Vidovic, D., et al., *Chem. Commun.*, 2010, vol. 46, p. 8546.

28. Fedushkin, I.L., Sokolov, V.G., Makarov, V.M., et al., *Russ. Chem. Bull.*, 2016, no. 6, p. 1495.
29. Fedushkin, I.L., Lukoyanov, A.N., Tishkina, A.N., et al., *Organometallics*, 2011, vol. 30, p. 3628.
30. Fedushkin, I.L., Sokolov, V.G., Piskunov, A.V., et al., *Chem. Commun.*, 2014, vol. 50, p. 10108.
31. Jones, C., Mills, D.P., Rose, R.P., Stasch, A., and Woodul, W.D., *J. Organomet. Chem.*, 2010, vol. 695, p. 2410.
32. Bonello, O., Jones, C., Stasch, A., and Woodul, W.D., *Organometallics*, 2010, vol. 29, p. 4914.
33. Gendy, C., Mansikkamaki, A., Valjus, J., et al., *Angew. Chem., Int. Ed.*, 2019, vol. 58, p. 154.
34. Protchenko, A.V., Dange, D., Schwarz, A.D., et al., *Chem. Commun.*, 2014, vol. 50, p. 3841.
35. Piskunov, A.V., Lado, A.V., Ilyakina, E.V., et al., *J. Organomet. Chem.*, 2008, vol. 693, no. 1, p. 128.
36. Klosener, J., Wiesemann, M., Niemann, M., et al., *Chem.-Eur. J.*, 2018, vol. 24, p. 4412.
37. Veith, M., Stahl, L., and Huch, V., *Organometallics*, 1993, vol. 12, no. 5, p. 1914.
38. Neto, J.L., de Lima, G.M., Porto, A.O., et al., *J. Mol. Struct.*, 2006, vol. 782, nos. 2–3, p. 110.
39. Jones, C., Stasch, A., and Woodul, W.D., *Chem. Commun.*, 2009, vol. 1, p. 113.
40. Sanden, T., Gamer, M.T., Fagin, A.A., et al., *Organometallics*, 2012, vol. 31, no. 11, p. 4331.
41. Arnold, P.L., Liddle, S.T., McMaster, J., et al., *J. Am. Chem. Soc.*, 2007, vol. 129, no. 17, p. 5360.
42. Hsueh-Ju, Liu, Ziegler, M.S., and Don Tilley, T., *Angew. Chem., Int. Ed. Engl.*, 2015, no. 54, p. 6622.
43. Arsenyeva, K.V., Ershova, I.V., Chegerev, M.G., et al., *J. Organomet. Chem.*, 2020, vol. 927, p. 121524.
44. Chegerev, M.G., Piskunov, A.V., Tsys, K.V., et al., *Eur. J. Inorg. Chem.*, 2019, p. 875.
45. Gordon, A. and Ford, R., *The Chemist's Companion: A Handbook of Practical Data, Techniques, and References*, New York: Wiley, 1972.
46. Arsenyeva, K.V., Chegerev, M.G., Cherkasov, A.V., et al., *Mendeleev Commun.*, 2021, vol. 31, p. 330.
47. *Handbook of Preparative Inorganic Chemistry*, Brauer, G., Ed., New York: Academic, 1991.
48. Piper, T.S. and Wilkinson, G., *J. Inorg. Nucl. Chem.*, 1956, vol. 3, p. 104.
49. Lado, A.V., Piskunov, A.V., Zhdanovich, I.V., et al., *Russ. J. Coord. Chem.*, 2008, vol. 34, no. 4, p. 251. https://doi.org/10.1134/S1070328408040027
50. *Smart. APEX3*, Madison: Bruker AXS Inc., 2018.
51. Krause, L., Herbst-Irmer, R., Sheldrick, G.M., and Stalke, D., *J. Appl. Crystallogr.*, 2015, vol. 48, p. 3.
52. Sheldrick, G.M., *Acta Crystallogr., Sect. C: Struct. Chem.*, 2015, vol. 71, p. 3.
53. Sheldrick, G.M., *Acta Crystallogr., Sect. A: Found. Adv.*, 2015, vol. 71, p. 3.
54. Holt, M.S., Wilson, W.L., and Nelson, J.H., *Chem. Rev.*, 1989, vol. 89, p. 11.
55. Piskunov, A.V., Aivaz'yan, I.A., Poddel'sky, A.I., et al., *Eur. J. Inorg. Chem.*, 2008, vol. 9, p. 1435.
56. Chegerev, M.G., Piskunov, A.V., Starikova, A.A., et al., *Eur. J. Inorg. Chem.*, 2018, p. 1087.
57. Chegerev, M.G., Piskunov, A.V., Maleeva, A.V., et al., *Eur. J. Inorg. Chem.*, 2016, p. 3813.
58. Tsys, K.V., Chegerev, M.G., Pashanova, K.I., et al., *Inorg. Chim. Acta*, 2019, vol. 490, p. 220.
59. Filippou, A.C., Winter, J.G., Kociok-Köhn, G., and Hinz, I., *Dalton Trans.*, 1998, vol. 12, p. 2029.
60. Titova, S.N., Bychkov, V.T., Domrachev, G.A., et al., *J. Organomet. Chem.*, 1980, vol. 18, no. 2, p. 167.
61. Pankratov, L.V., Nevodchikov, V.I., Zakharov, L.N., et al., *J. Organomet. Chem.*, 1992, vol. 429, no. 1, p. 13.
62. Veith, M. and Stahl, L., *Angew. Chem., Int. Ed. Engl.*, 1993, vol. 32, no. 1, p. 106.

*Translated by E. Yablonskaya*